Neural Computing and Applications
https://doi.org/10.1007/s00521-022-07229-x

ORIGINAL ARTICLE

Patient activity recognition using radar sensors and machine learning

Geethika Bhavanasi[1] · Lorin Werthen-Brabants[1] · Tom Dhaene[1] · Ivo Couckuyt[1]

Received: 5 October 2020 / Accepted: 29 March 2022

Abstract
Indoor human activity recognition is actively studied as part of creating various intelligent systems with applications in smart home and office, smart health, internet of things, etc. Intrusive devices such as video cameras or sensors attached to the human body are often used to realize human activity recognition. These solutions, however, lead to various privacy issues. On the other hand, radar sensors are privacy-preserving and provide a lot of information about the subject such as speed, distance, range, and angle. Moreover, radar sensors can sense through the walls. In this respect, we investigate the use of radar data to achieve patient activity recognition. In particular, human activity data are collected from both an indoor environment that replicates a hospital setting and a real-life hospital room using two high dimensional radar sensors. The data are further fed to various supervised Machine Learning (ML) classification approaches. We investigate the robustness and generalization capabilities of the ML approaches with respect to people's age, radar sensor position, mobility aids and environments. The results show promising levels of accuracy. The Convolutional Neural Network (CNN) using Micro-Doppler (MD) maps are more effective for generalizing across different environments and radar positions with 62% and 73% accuracy, respectively. The CNNs using Range-Doppler (RD) maps are more efficient than using MD maps within the same environment in the case of distribution of age (87–95%), mobility aids (91–95%) and with different subjects (93–95%). A subset of the data set is made publicly available.

Keywords Human activity recognition · Patient monitoring · Machine learning · Radar sensors

1 Introduction

Healthcare systems of today are facing two serious challenges: rapid growth of the elderly population and severe shortage of medical practitioners [1]. Nowadays, patients are increasingly monitored using devices ranging from various medical sensors to typical Internet of Things (IoT) sensors. Indoor human activity recognition is one of the vital aspects of many intelligent surveillance systems ranging from smart homes to patient health monitoring tools. These surveillance systems commonly use video cameras as their primary sensors. Video-based surveillance systems have advantages such as wide viewing angles, high-definition resolution, and cost-effective. However, they show fundamental deficiencies such as being inefficient in poor weather and low-light environments, more difficult to detect subjects with concealing clothes, etc.

Moreover, video-based sensors are intrusive, and may not be a feasible choice where privacy plays an important role. In contrast, radar devices can operate in a variety of severe conditions such as rain, fog, dust, darkness, smoke, and heat. Further, radar devices are privacy-preserving and non-intrusive in their nature which facilitate their usage in environments with a high privacy-demand. In addition, they are capable of sensing through the walls or any other obstructing elements [2]. These qualities of the radar sensors make them a logical choice for indoor human activity recognition where privacy plays a significant role. Hence, modern and compact radar sensors are an interesting option as an alternative to video cameras in many applications today.

A radar device transmits an electromagnetic radio signal in its line of sight that gets reflected by targets and objects. The reflected signal is then captured by the receiver after a certain time delay. The received signal is used to calculate

✉ Geethika Bhavanasi
Geethika.Bhavanasi@ugent.be

[1] Department of Information Technology (INTEC), Internet Technology and Data Science Lab (IDLab) Research Group,iGent, Ghent University–imec, Technologiepark-Zwijnaarde 126, 9052 Ghent, Belgium

Published online: 03 May 2022

the range and angle of the target. If the target is moving, then the frequency shift in the received signal can be used to estimate the speed of the moving object [3, 4]. If there are many independently moving objects, the superposition of all the reflected signals can be represented as a Micro-Doppler (MD) signature [5].

In this paper, we present Machine Learning (ML) approaches for indoor human activity recognition using Frequency Modulation Continuous Wave (FMCW) radars (77 GHz and 60 GHz) and a video camera, where the latter is only used for validation and annotation. In particular, we monitor patients or elderly people by recognizing different activities in a hospital room by using the radar sensors in a non-intrusive way. To the best of our knowledge, there are no public radar data sets that contain activities recorded simultaneously with multiple radar sensors in a hospital room. The summary of the main contribution of our research are as follows:

1 *Data collection in hospital rooms:* Two extensive data sets are constructed which include indoor patient activities from two different types of environments: a synthetic hospital room and a real-life hospital room. A part of these two data sets is made publicly available as *PARrad (Patient Activity Recognition with Radar sensors)*[1], in order to allow benchmarking and to facilitate further research activities in this direction.
2 *Neural Network architecture:* we propose a robust deep learning architecture that is able to recognize patient activities effectively. We compare against other supervised classification models such as Convolutional Neural Network-Long Short-Term Memory (CNN-LSTM), LSTM, Support Vector Machine (SVM), Linear Discriminant Analysis (LDA), and Random Forest (RF).
3 *Effect of different ML models and radar data:* we compare the effectiveness of various ML models using radar data from two different environments. We also demonstrate how the ability of the ML models vary in predicting patient activities when two different kinds of data, known as MD signatures and Range-Doppler (RD) maps, that originate from high dimensional sensors are used as the input to ML models.
4 *Robustness:* we investigate the robustness with respect to people's age (adult vs elderly people), mobility aids (without any aids vs with aids: walking stick and walker), radar position (77 GHz vs 60 GHz radar sensors) and environments (Hospital vs Homelab).

The rest of the paper is organised as follows: in Sect. 2, we presented a brief overview on related work on indoor human activity recognition with different sensors. In Sects. 3 and 4, an overview of the utilised sensors and the machine learning algorithms are presented, respectively. In Sect. 5, our proposed approach is detailed and the experimental setup used to validate our approach is discussed. In Sect. 6 contains a detailed discussion of our experimental results. Finally, in Sect. 7, we conclude our work and provide potential directions for future research.

2 Background and related work

Human activity recognition is extensively investigated for many intelligent systems such as smart homes and smart health. [6]. Human activities range from simple to complex movements such as using a single hand to open the door, or running, that causes movement of legs, arms and the whole body. In most of the applications, video cameras are commonly used to monitor human activities. Starting from motion detection to activity recognition, various neural network models are investigated [7–10]. In [11], different architectures of CNN are investigated to learn the spatial and the temporal information from a large-scale video data set. LSTM and feature pooling methods are presented in [12] for better classification of lengthy video data sets. In [13], Three Dimensional (3D)-CNN outperforms two Dimensional (2D)-CNN in learning the spatio-temporal features from videos. These research activities are followed by an extensive study of human activity recognition with deep learning [14–19].

The population of elderly people is significantly growing worldwide [1]. Elderly people or patients show decline in day-to-day physical activities due to physical and mental deterioration caused by ageing [20]. The safety of elderly people can be improved by monitoring their daily activity patterns. The monitoring process may enable us to identify the occurrence of critical life changing events. Over the last few years, extensive research efforts are carried out on a wide variety of devices to monitor elderly people and to enhance their independent life. Sian Lun Lau et al. [21] created a movement recognition assistant named CARMA powered by smartphone with a built-in accelerometer and ML methods like Decision Tree, K- nearest neighbours, etc. In [22], accelerometer and decision tree algorithms are used to detect 10 falling movements of Transient Ischemic Attack patients. The authors used IoT technology that notifies the patients family to take immediate action if the patient has fallen. Lisa Schrader et al. [23] investigated the changes in physical activities of elderly people and patients by creating a data repository of various activities under different environmental conditions using various wearable and ambient sensors. The authors used RF algorithms to recognize the activity patterns. In the health care sector,

[1] The data set is publicly available at: https://www.imec-int.com/en/PARrad.

various sensors and methods are investigated to advance the healthcare services which aim to provide support to patients and elderly people [24–28].

In recent years, the use of non-intrusive and non-wearable devices for human activity recognition is explored. Unlike cameras or wearable sensors, radars ensure comfort by their contact-less and non-invasive properties (i.e., people do not need to wear, interact or carry radar sensors). Hence, radar devices are often preferred in intelligent surveillance systems where privacy is an important factor (e.g., indoors, hospital rooms, etc.) [29–34]. Google designed a mm-wave radar system Soli and used signal processing and machine learning techniques to recognize finger gestures [35, 36]. Baptist Vandersmissen et al. [37] used high dimensional sensors (77 GHz FMCW radar and camera) to recognize various human gestures and events. As part of the work, the authors created two data sets with 6 different types of gestures and events. This research shows that a sensor fusion approach with CNN-RD considering radar RD maps is a promising approach for human activity recognition.

When it comes to the healthcare sector, radar sensors are essentially used in monitoring daily physical activities [38, 39] and vital signs [40] in order to improve the physical and the cognitive well-being of patients. Francesco Fioranelli et al. [41] use radar sensors for multiple purposes in order to fulfil the needs of the healthcare system. Radars are often investigated for activity recognition to ensure immediate medical treatment for patients in case of life changing events [42–44]. In [45], radar data with both range and velocity information are used for fall detection. Li et al. [46] focus on both magnetic and radar sensors to monitor 10 different daily activities of 20 subjects and next, various classification algorithms are used to achieve both fall detection and activity classification.

Mu Jia et al. [47] explore the robustness of different ML algorithms (SVM, Stacked AutoEncoder (SAE) and CNN) for recognizing 6 different human activities (using a FMCW radar operating at 5.8 GHz with 400 MHz bandwidth and 1ms chirp duration [38, 48]). Besides, RD and MD maps, 2 more features are extracted from the radar data: a phase diagram and a cadence velocity diagram. The classification accuracy of over 96% is achieved by the feature fusion of handcrafted features and CNN features (obtained from MD input).

There are existing radar data sets which are publicly available. The *"Radar signatures of human activities"* data set contains 6 different indoor human activities (walking, sitting down, standing up, pick up an object, drink water and fall) performed by several people at different locations (collected with a 5.8 GHz FMCW radar) [38, 48]. A *"DopNET radar micro-Doppler"* database is introduced by the UCL Radar Research Group, where the data set contains 4 different hand gestures (swipe, wave, pinch and click) recorded with a 24 GHz FMCW radar [49]. The *"Human Activity Recognition with a Radar"* (HARrad) data set with 6 different types of hand gestures and indoor human activities (collected using a 77 GHz FMCW radar) is mentioned in [37]. The *"Indoor person identification with a Radar"* (IDRad) data set contains 150 min of MD signatures of walking activity (collected using a 77 GHz FMCW radar) performed by 5 subjects [50].

Most of the above mentioned research works share that the experiments are mostly conducted in well-controlled environments. The data sets in our work are more specific to the patient activities in a hospital room as compared to many of the publicly available data sets. Moreover, the activities in one of our data sets are collected in a real hospital environment (which is a less controlled setting). The two high dimensional FMCW radar sensors are higher in frequency (77 GHz and 60 GHz), bandwidth (1.536 GHz) and range resolution (9.77 cm) (see Table 1) as compared to other public data sets. Moreover, we use two different radar sensors to investigate the robustness of ML approaches with respect to different radar positions. Furthermore, the human activities are focused on patient activities with mobility aids (walking stick and walker) in the hospital room and we include fine-grained small motion activities (i.e., bed activities).

3 Radar sensors fundamentals

The Texas Instruments (TI) Millimeter (Mm) Wave FMCW radars set up in Multiple Input Multiple Output (MIMO) mode are used [4]. In particular, the xWR14xx (77 GHz) and xWR68xx (60 GHz) sensors, originally developed for the automotive sector. These radars have the added advantage of exhibiting high power efficiency while at the same time being able to be produced at low-cost. However, the high power efficiency comes at the cost of having an inferior Signal to Noise Ratio (SNR) [51] that often poses significant challenges in analysing the data.

The FMCW radar is an active sensor that continuously emits electromagnetic signals through a transmitting antennas which gets reflected by the target and captured by an array of receiving antennas [3, 4]. Essential information about the targets (such as range, angle, and speed) are then extracted from the reflections based on the time delay or phase shift (i.e., the Doppler effect [52]). The RD maps, which give information on the range and the velocity of the target, are generated by applying the 2D Fourier transforms on the reflected signals [5]. A MD signature is obtained from RD maps by summarizing over the range dimension

Table 1 TI MmWave FMCW radar configuration recording parameters

	Radar-1	Radar-2
Device		
Device type	xWR14xx	xWR68xx
Lower frequency	77 GHz	60 GHz
Maximum bandwidth	4 GHz	4 GHz
Max. number of Rx	4	4
Max. number of Tx	3	3
Configured parameters		
Centre frequency	77.89 GHz	61.14 GHz
Sampling frequency	5.00 MHz	5.00 MHz
Radar bandwidth	1.536 GHz	1.536 GHz
Data bandwidth	134 Mb/s	134 Mb/s
Chirp period	8e-05 s	8e-05 s
Chirp loops	128	128
Frame period	90.0 ms	90.0 ms
Frame rate	11.1 fps	11.1 fps
Frame gap	59.3 ms	59.3 ms
Frequency slope	30	30
Receiving antennas (Rx)	4	4
Transmitting antennas (Tx)	3	3
Range bins	93	93
Doppler bins	128	128
Max. velocity	4.01 m/s	5.11 m/s
Velocity resolution	0.06 m/s	0.08 m/s
Max. range	22.50 m	22.50 m
Range resolution	9.77 cm	9.77 cm
MIMO mode	Yes	Yes

and concatenating over the time dimension. Figure 1 shows examples of MD signatures and RD maps of different activities. These activities are performed by the patients in a hospital room which are recorded by the sensors employed in this work. Moreover, we used the video sensor for the sole purpose of validation and annotation.

4 Machine learning algorithms

We focus on *Deep Convolutional Neural Networks (DCNNs)*, and we compare their performance with other deep learning and traditional modeling pipelines (i.e., LSTM, CNN-LSTM, SVM [53], LDA and RF [54] classifiers). Figure 8 shows our neural network architectures which are described in Sect. 5.3.1.

A DCNN is composed of various components such as convolutional layers, activation functions, and pooling layers. The architecture of a given DCNN is decided by the way its components are interconnected. Through the convolutional process, see Fig. 2, in each layer multiple convolutional filters work in parallel for feature mapping which refers to the idea that each convolutional filter can be trained to search for different features in an spectrogram or image, which can then be used in the classification process [55]. Hence, each convolution filter is a specific feature detector. The nonlinear activation function performed on the output of a convolution filter enables a nonlinear transformation of the data which helps more easily to discriminate among classes, i.e., it represents the nonlinear connection between inputs and outputs. There are many activation functions in use such as sigmoid, Exponential Linear Unit (ELU), and Rectifier Linear Units (ReLU) [56].

Using ReLU and ELU activation function was shown to solve the vanishing gradient problem [57, 58]. The next component pooling layer is another sliding window type technique which reduces data dimensions by down sampling the image, which enables the final prediction to be more robust to noise. The pooling can be performed by choosing either maximum value (max pooling) or mean value (average pooling). The most common type of pooling is max pooling which applies the max() function over the window contents as shown in Fig. 3. In addition, dropout is used as a regularization scheme, to avoid overfitting. Finally, we have a fully connected layer which can be thought of as a standard classifier attached to the output of the network to make predictions.

5 Methodology

The main objective of this research work is to recognize various activities performed by persons in indoor environments using FMCW radar sensors. Figure 4 shows the schematic overview of the proposed approach. The DCNNs are used to automatically recognize various human activities in hospital rooms. In this respect, two data sets are created using two high dimensional radar sensors with separate nominal frequencies. The data sets contain 21859 (time-series) samples for 10 activities of 29 subjects. The data collection is carried out in two environments: a synthetic hospital room and a real-life hospital room. In particular, we address the following key areas:

1 The effect of using various forms of data emanating from the radar sensors on the accuracy of the ML models built with the proposed DCNN architectures.
2 The robustness with respect to different environments, people's age, mobility aids and radar position.

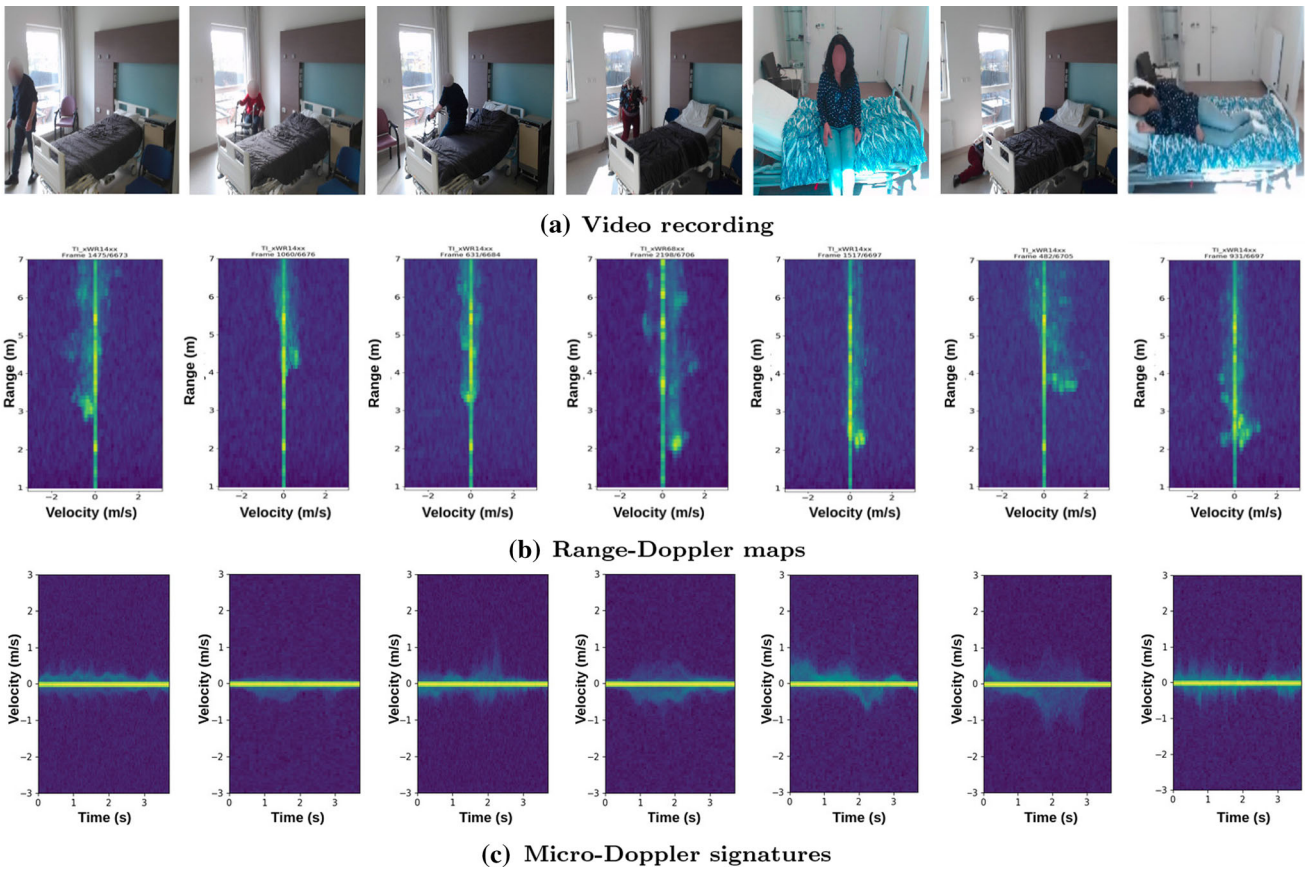

Fig. 1 Radar data of different activities labelled as: walk to room, sit down on chair, get in bed, walk to bed, sit down on bed, fall on the floor and roll in bed. In **a** a video recording, **b** and **c** related radar recording: Range-Doppler (RD) maps and Micro-Doppler(MD) signatures respectively

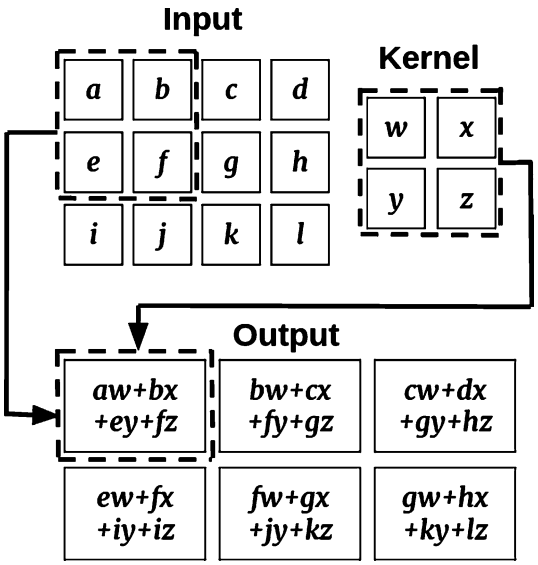

Fig. 2 Example of a two-dimensional convolutional operation. A 2×2-sized kernel is used to perform convolution on a 3×4-sized input with zero padding to produce an output feature map. The operation of each element is shown in the resulting output feature map

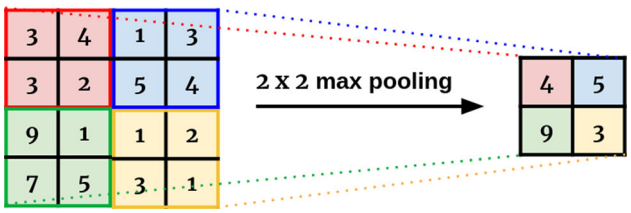

Fig. 3 Example of a two-dimensional max pooling operation with size 2×2 filters and stride 2. A 4×4-dimensional feature map is reduced to a 2×2-dimensional feature map by selecting the maximum value of each 2×2 subregion

5.1 Experimental setup

5.1.1 Data set

Data collection is performed in two different environments: Homelab and Hospital. Both environments are about 30 m^2 (Fig. 5). As discussed earlier, we are monitoring the patients in the hospital room by recognizing different activities in an non-intrusive way and ensuring patient comfort. For this reason, we collect data for different patient activities with two different FMCW radar devices and a webcam, in two separate environments.

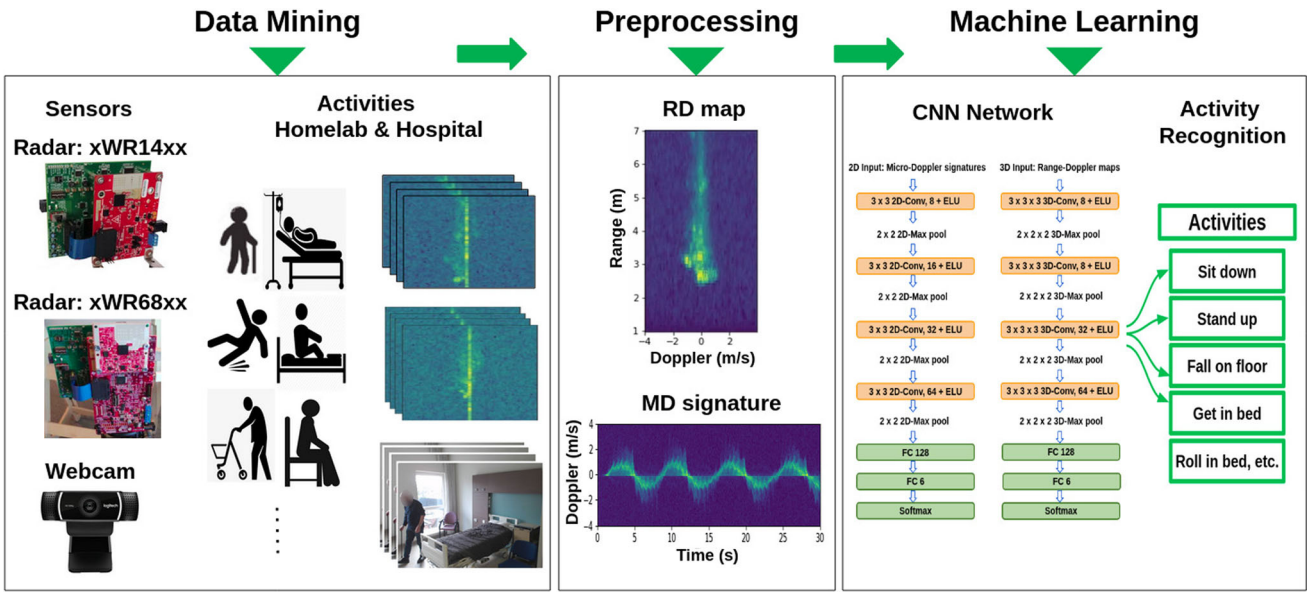

Fig. 4 Schematic overview of the proposed approach for the Homelab and the Hospital data sets

Fig. 5 Data collection: The 77 GHz radar is placed near the ceiling, while the 60 GHz radar and webcam are placed at eye-level height on a tripod

Table 2 Overview of 14 different patient activities in both Homelab and Hospital data sets

	Total samples	Avg. time (s)
In-room activities		
Walk to room	2053	4.0
Fall on the floor	1782	3.6
Stand up from the floor	1772	4.0
Walk to chair	2102	3.4
Sit down on chair	1854	2.5
Stand up from chair	1820	2.5
Walk to bed	2384	4.1
Sit down on bed	921	3.0
Stand up from bed	895	2.5
Bed activities		
Get in bed	1300	3.5
Lie in bed	1153	2.6
Roll in bed	1148	5.0
Sit in bed	1145	2.5
Get out bed	1240	3.6

The intention of using more than one radar sensor is to improve the robustness of the model by placing each radar in different positions. In addition to providing more data, placing radars at different locations enables us to recognize the same set of activities with different values of radar data. The detailed radar recording parameters that are used for the data collection in both environments are given in Table 1.

In order to easily record the activities, we have provided the subjects with audio of the activity to be performed, with a display mentioning the current activity (+ a timer), and also the next upcoming activity, so that the subject clearly knows which particular activity to perform at any time. We have recorded 14 different activities, summarized in Table 2. We group similar activities as shown below:

- walk to bed, walk to room, walk to chair –> walk
- sit down on bed, sit down on chair –> sit down
- stand up from bed, stand up from chair –> stand up

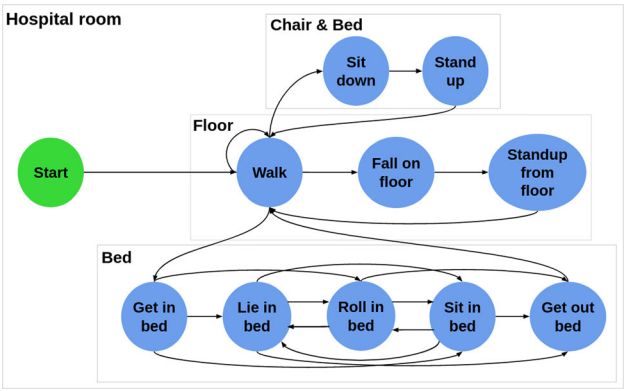

Fig. 6 Different activities performed in hospital room and the connectivity between them

Thus, the 14 original activities are grouped into 10 different classes of activities. Moreover, the 10 classes of activities are consecutive as depicted in Fig. 6. For instance,"walk –> walk, fall on the floor, sit down, get in bed"represents the following consecutive actions: if the current activity of a person is walking then the next activity can be either walk or fall on the floor or sit down or get in bed.

5.1.2 Homelab environment

Homelab[2] is a unique standalone residential test environment of 240 square meters for IoT applications. We have modified one of the rooms of the Homelab in such a way that it acts as a hospital room. This synthetic hospital room consists of a hospital bed, a chair, two tables, a cupboard and a bathroom. We have recorded 9 different subjects which involve all adult people. The 77 GHz radar sensor was fixed near the ceiling in one corner of the room, the 60 GHz radar sensor and the webcam are positioned at eye-level height. All the three sensors are placed on the same side of the room as shown in Fig. 5. Moreover, the sensors are directed towards the main entrance of the room so that they cover the whole room. The recording was done in four sessions and the duration of each session was 10 minutes with randomly chosen activities. Thus, each subject recorded continuously in these four sessions, during which they performed all the specified actions.

5.1.3 Hospital environment

A real-life hospital room in a local hospital is used. The data set is composed of both elderly and adult people (i.e., synthetic patients) performing different activities. We have recorded 20 different subjects. As shown in Fig. 5 , the two radar sensors are placed at two different corners with the radar 77 GHz almost near the ceiling and the radar 60 GHz at slightly above average eye-level height whereas the webcam is placed near the 77 GHz radar. In this environment, we have a hospital bed, 3 chairs, other hospital related materials, cupboards, a table, a sink room and a bathroom. Similar to Homelab data collection, the recording is done in four sessions with each 10 min random activities. For each session we changed the position of chairs and out of four sessions, two sessions involve activities using mobility aids: walking stick and walker. Moreover, we have done some manual cleanup of the data as we encountered the following challenges in this environment:

- Some elderly people could not perform"*fall on the floor*"and" *stand up from the floor*"activities (see Table 11).
- Some activities had a duration of less than 2 s.

The activities involved in the above mentioned cases are removed from the final data sets. Therefore, the final data sets contain 21569 activities, subdivided into 8210 Homelab activities and 13359 Hospital activities. The data sets thus contain a total of 22 h of data which is effectively annotated and distributed over 10 activity classes. Furthermore, the speeds of the subjects are different for different activities as it involves adult and elderly people. As the activities are randomly generated for each section and for each subject, the number of samples is unequal for different activities. In Hospital data, we have adult people, elderly people, with mobility aids (walking stick and walker), without mobility aids and combination of all of them. Whereas, in Homelab data, we have only adult people without mobility aids. An overview of the recorded activities in Homelab and Hospital rooms is given in Table 3. Tables 10 and 11 list some of the basic information of the participants in Homelab and Hospital data sets, respectively. All of our participants are aged between 24 and 90 years. Their heights and weights range from 155 to 185 cm and from 47 to 95 kg, respectively.

5.2 Pre-processing

5.2.1 Range and Doppler dimensions

The RD map is obtained by applying the 2D Fourier transform to the raw radar data, and then converting the absolute values of the RD signal to decibels (dB). The RD map is three dimensional, which contains range, Doppler and time units, with 93 range bins (0.9 to 9.9 m), and 128 Doppler bins (− 4.0 to +3.9 m/s). The MD is the summation of the RD maps over the range dimension. We

[2] https://www.ugent.be/ea/idlab/en/research/research-infrastructure/homelab.htm.

Table 3 The number of samples for each activity in different data types

Data types	Activities										
	Walk	Sit down	Stand up	Fall on the floor	Stand up from the floor	Get in bed	Lie in bed	Roll in bed	Sit in bed	Get out bed	Total
Homelab	2412	966	932	690	690	548	490	494	476	512	8210
Hospital	4127	1809	1783	1092	1082	752	663	654	669	728	13,359
Hospital without any aids	2213	1013	949	570	562	406	371	368	363	389	7204
Hospital walking stick	1088	486	482	296	292	196	166	152	166	190	3514
Hospital walker	1052	460	452	278	278	188	170	168	172	182	3400
Hospital elderly people	1646	726	718	390	386	292	238	258	258	282	5194
Hospital adult people	2481	1083	1065	702	696	460	425	396	411	446	8165
Hospital adult without any aids	1111	475	467	314	310	206	197	196	185	198	3659
Hospital radar 77 GHz	2047	896	883	541	536	374	329	325	332	362	6625
Hospital radar 60 GHz	2080	913	900	551	546	378	334	329	337	366	6734

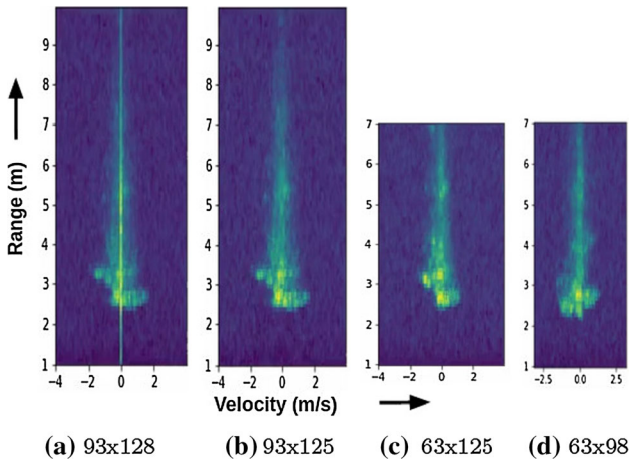

Fig. 7 Visualization of an example RD map fed as input to our model: **a** Original RD map with 93 range and 128 Doppler bins, **b** Remove static (centre) Doppler bins, **c** Remove range bins, and **d** Remove outer Doppler bins

reduced the dimensions of each MD signatures and RD maps to 98 and 63x98 respectively.

In the Doppler dimension, we remove both zero-Doppler bins and outer-Doppler bins. The three middle Doppler bins which represent all static objects with zero velocity are removed without loss of any pertinent information [50]. In case of the outer-Doppler bins we empirically decided to remove the 13 Doppler bins on one side and 14 Doppler bins on the other side, corresponding to velocity ranging from -3.1 to $+3.1$ m/s. In a similar way, in the range dimension, we observe that the performed activities of the subjects are up to 7 m as per the size of the room in both the environments. For this reason, we remove the outer range bins and thus eliminating any external noise signals that are not in the range of a hospital room. At the end, we have 98 Doppler and 63 range bins as shown in Fig. 7.

5.2.2 Sample length

A sample is a set of consecutive frames which contains the complete activity of the target. The recordings are labelled by segmenting the radar frames based on the activity audio and the radar timestamps. Additionally, we use video data timestamps for validating the annotation. The optimal sample length is 40 frames, i.e., 3.7 seconds, based on performing analysis on different sample lengths. Moreover, we also consider a padding where if the sample length is less than a specified k seconds, we pad with the last frame to fill the rest of the frames. The range, Doppler and time dimensions are given in Table 4.

5.3 Modelling

5.3.1 Models

We create two neural network architectures using the PyTorch[3] machine learning framework. One which accepts the 2D-MD signatures, and the other which accepts the 3D-RD maps. Each network consists of convolutional layers, activation function, pooling and fully connected layers. The architecture CNN-MD takes two-dimensional MD signatures as input data. We used four convolution layers. The CNN-MD network extracts features from the Doppler and the time dimensions by using the two-dimensional convolutional layers with 8, 16, 32 and 64 convolutional

[3] https://pytorch.org.

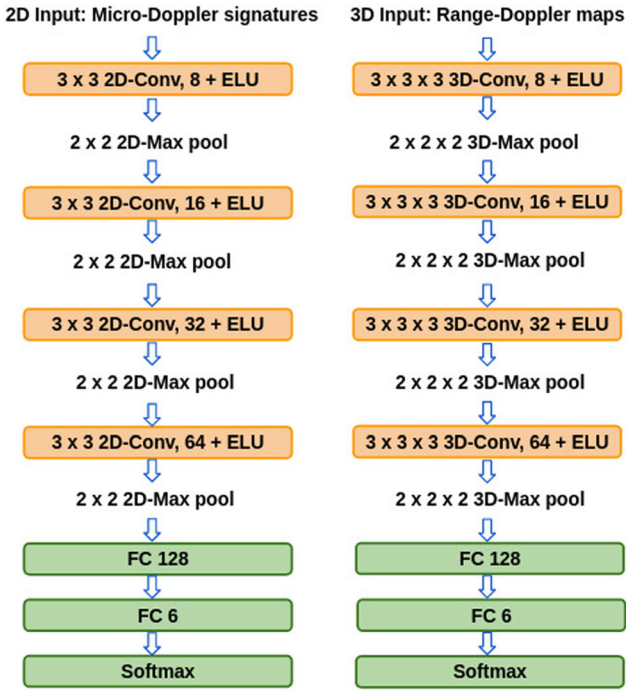

Fig. 8 Convolutional neural network (CNN-MD and CNN-RD) architectures

filters, respectively. Further, to reduce the input data dimensions, each convolutional layer is followed by a non-overlapping max pooling layer of size 2x2. Finally, predictions are made by the network based on two fully connected layers of size 128 and 6, respectively.

To prevent the network from overfitting, dropout is performed at an increasing rate to all the layers except the last fully connected layer. The activation function ELU is used to introduce a nonlinearity operation which is often followed by convolutional and fully connected layers. ELU is defined as follows:

$$ELU: \mathrm{f}(x;\alpha) = \begin{cases} x, & \text{if} \quad x > 0 \\ \alpha * (e^x - 1), & \text{if} \quad x \leq 0 \end{cases}$$

with $x \in \mathbb{R}$ represents the input and α a predefined parameter greater than zero. The softmax nonlinearity is used by the last fully connected layer to get probabilities for each target class. The architecture CNN-RD takes three-dimensional RD maps as input. The CNN-RD is similar to CNN-MD network, with one dimension more for both the convolutional and pooling layers. Both network architectures are shown in Fig. 8. We adapt other deep learning architectures from [37]. In total, we compare against four additional architectures: (i) LSTM-MD and CNN-LSTM-MD networks which take MD signatures as input and (ii) LSTM-RD and CNN-LSTM-RD networks which take RD maps as input. The other ML algorithms we have used in this research work are SVM, LDA and RF, from the Scikit-learn[4] machine learning library.

Table 4 Learning parameters of the deep learning models: convolutional neural network (CNN), long short-term memory (LSTM) and CNN-LSTM

Parameters	Values
Sample length	$k = 3.7$ s $\equiv$ 40 frames
Range dimension	7 m $\equiv$ 63 bins
Doppler dimension	-3.1 to $+3.1$ m/s $\equiv$ 98 bins
Epochs	2000
Batch size	256
Optimizer	Adam optimizer
Learning rate	10^{-3}
Loss function	Cross-entropy loss
Mini-batches	64
Normalization	Mean and standard deviation
Padding approach	With last frame

5.4 Learning

The neural network models are trained for 2000 epochs with a batch size of 256, making sure the classes are balanced for each mini-batch. It takes around 2 hours (MD) and 8 hours (RD) on average to converge (using a GeForce GTX 1080, TITAN X and GeForce RTX 2080 Ti graphic cards), but it always depends on the data we are using to train the model. For the given data sets, 80% of the data of each target were used as training data set, and the other 20% were used as validation data set. The test data set varies according to what type of generalization we are testing (mobility aid, environment, etc.). The learning parameters used for the deep learning models are given in Table 4. For robust modelling and data diversity, in the training phase, we have randomly selected the frames of a sample for the specified sample time range of k seconds. In the training, validation and test phase, if the sample is less than this time range, we performed padding with the last frame. The details of the parameters of SVM, RF and LDA used in both training and testing phase are given in Table 5.

5.5 Evaluation

We evaluate the trained model by computing the error rate that is calculating the wrongly classified samples out of the total test samples. We consider two approaches for prediction of the activity of the sample: Normal (N) prediction and Ensemble (E) prediction. In the normal case, a sample of k seconds is cropped from the middle frames of the

[4] https://scikit-learn.org.

Table 5 Hyperparameters of the support vector machine (SVM), linear discriminant analysis (LDA) and random forest (RF) models

Algorithm	Parameters
SVM	Optimization: grid search CV
	Regularization C: [0.1, 1, 10, 100]
	Gamma MD: [0.001, 0.01, 0.1]
	Gamma RD: [0.000001, 0.000004, 0.00001]
	Kernel: radial basis function (rbf)
	Class weight: balanced
	Cross validation (CV): 5 folds
	All other parameters: default
LDA	Solver: singular value decomposition (svd)
	All other parameters: default
RF	Optimization: grid search CV
	Max features: auto
	Bootstrap: True
	Class weight: balanced
	Cross validation (CV): 5 folds
	Max depth: [30, 40, 50, 60, 70, 80]
	Min samples leaf: [3, 4, 5]
	Min samples split: [8, 10, 12]
	Estimators: [500, 1000, 1500, 2000]
	All other parameters: default

whole time range. In the ensemble case, we aggregate many normal predictions using a majority vote. Similar to the training process, we extended each sample that is shorter than this time range, with the padding approach. The generalization of the models are evaluated in a stratified leave-one-out approach, where we use the following test set and the model is each time trained on the remaining data:

1 People's age and mobility
   - Adult people and elderly people

2 Mobility aids
   - With mobility aids (walking stick and walker)
   - Without any aids

3 Environments
   - Hospital and Homelab

4 Subjects
   - Leave-five-subjects out

5 Radars
   - 77 GHz and 60 GHz

For all results, the performance metrics we consider are precision, recall, f1-score and accuracy.

6 Results

6.1 People's age and mobility aids (Hospital)

The results are shown in Table 6 *Case-1*. The proposed models trained with adult people data and tested on elderly people data obtain an accuracy of 92% for the CNN-MD network and 95% for the CNN-RD network. The vice versa of this case gave a model performance of 80% and 87% accuracy for the CNN-MD and the CNN-RD networks, respectively. The reduction of model performance can be explained by the data set of the elderly people being smaller than the adult people data set. Similarly, the model trained without mobility aids data and tested on walking stick and walker data results in a high performance of 95% and 91% accuracy for the CNN-RD network, respectively. Alternatively, testing on adult people data and without mobility aids data exhibit similar accuracy levels. The other ML algorithms SVM, LDA and RF have results that correlate with the findings above, but are clearly lower than the CNN models. For all these cases, we conclude that the CNN-RD network is the best performing setup, with both range and Doppler features (RD maps) as input.

6.2 Environments (Hospital and Homelab)

The results of all the algorithms are given in Table 6 *Case-2*. The Homelab data set contains only adult people without mobility aids samples (as discussed in Sect. 5.1.1). The radar-based models, CNN-MD and CNN-RD result in an accuracy of 62% and 45%, respectively.

6.3 Subjects (leave-five-subjects-out)

We discuss the results for 4-fold cross validation over 20 subjects. The confusion matrix of the CNN-RD network are given in Table 7. The results for each fold with different performance metrics are detailed in Table 8, which shows that the new subjects activities are predicted by models with an average accuracy of 89% (CNN-MD) and 95% (CNN-RD). The results for other ML algorithms are given in Table 9.

6.4 Radars (77 GHz and 60 GHz)

Finally, we show the results for generalization between the two radars considered in this work. While we expect the frequency difference to have little effect, the position of the radars could matter greatly for the model robustness. The models trained on Hospital radar 77 GHz samples and tested on Hospital radar 60 GHz samples obtained on

Table 6 Results of the model performance in terms of accuracy performance metrics for Case-1: the combinations of different data types in the Hospital environment, Case-2: model generalization considering two different environments and Case-3: model generalization considering two different radars (77 GHz and 60 GHz) in the Hospital environment, with different models: Convolutional Neural Network (CNN), Long Short-Term Memory (LSTM), CNN-LSTM, Support Vector Machine (SVM), Random Forest (RF), Linear Discriminant Analysis (LDA) and different radar input data: 2D input Micro-Doppler (MD) signatures and 3D input Range-Doppler (RD) maps and two prediction approaches for the CNN model: Normal (N) and Ensemble (E) (in the ensemble case 50 variants of samples are considered)

Model	Case-1		
	Train: without mobility aids		Train: adult people
	Test: walker (N, E)	Test: walking stick (N, E)	Test: elderly people (N, E)
CNN-MD	0.77, 0.78	0.84, 0.85	0.91, 0.92
CNN-RD	0.90, **0.91**	0.94, **0.95**	**0.95**, **0.95**
LSTM-MD	0.70, 0.72	0.78, 0.80	0.88, 0.88
LSTM-RD	0.82, 0.84	0.86, 0.87	0.91, 0.91
CNN-LSTM-MD	0.75, 0.77	0.82, 0.83	0.88, 0.89
CNN-LSTM-RD	0.87, 0.89	0.92, 0.93	0.93, 0.94
SVM-MD	0.66	0.73	0.81
SVM-RD	0.73	0.80	0.85
RF-MD	0.60	0.67	0.71
RF-RD	0.65	0.70	0.76
LDA-MD	0.30	0.31	0.39
LDA-RD	0.64	0.68	0.77

Model	Case-2	Case-3
	Train: Adult without mobility aids	Train: 77 GHz radar
	Test: Homelab	Test: 60 GHz Radar
	(N, E)	(N, E)
CNN-MD	0.59, **0.62**	0.71, **0.73**
CNN-RD	0.44, 0.45	0.65, 0.66
LSTM-MD	0.60, 0.61	0.62, 0.63
LSTM-RD	0.22, 0.24	0.51, 0.51
CNN-LSTM-MD	0.54, 0.56	0.67, 0.69
CNN-LSTM-RD	0.42, 0.43	0.60, 0.60
SVM-MD	0.46	0.57
SVM-RD	0.27	0.54
RF-MD	0.42	0.54
RF-RD	0.32	0.55
LDA-MD	0.21	0.34
LDA-RD	0.23	0.49

The best model for each test set is highlighted in bold

accuracy of 73% for CNN-MD and 66% for CNN-RD. All the results for this case are shown in Table 6 *Case-3*.

6.5 Comparison with other deep learning approaches

The results of the LSTMs and the CNN-LSTMs for all the different cases are given in Tables 6 and 9. Based on the results, we observe that the impact of both MD and RD in the LSTM and the CNN-LSTM models are similar to the CNN models. Moreover, the performance of CNN-LSTM with RD maps approaches our proposed CNN-RD network. Furthermore, in general, CNN-LSTM networks perform better than LSTM networks.

6.6 Final results

Based on the results of the different cases, we can clearly see that the CNN models are the best performing compared to other ML (LSTM, CNN-LSTM, SVM, LDA and RF) algorithms. Similar results are observed in [47], where CNNs with MD maps outperform SVM and SAE with 92% accuracy, and 77% accuracy when generalizing to other environments. In our work, we also investigated the use of

Table 7 The resulting confusion matrix for the Hospital data set after summing the confusion matrices of all splits of the leave-five-subjects-out cross validation. The predictions are obtained by the CNN-RD radar-based network

	Predicted label									
	Sit down	Stand up	Walk	Fall on the floor	Stand up from the floor	Lie in bed	Get in bed	Roll in bed	Get out bed	Sit in bed
True label										
Sit down	**1688**	8	28	38	9	7	27	1	2	1
Stand up	25	**1581**	34	2	68	0	0	1	70	2
Walk	27	20	**4052**	13	13	0	1	0	1	0
Fall on the floor	19	0	14	**1042**	12	4	1	0	0	0
Stand up from the floor	9	23	19	1	**1020**	1	1	1	5	2
Lie in bed	11	0	0	1	1	**599**	32	12	3	4
Get in bed	10	0	2	1	1	3	**716**	14	2	3
Roll in bed	1	0	2	0	3	9	7	**523**	3	8
Get out bed	3	31	1	0	0	1	1	3	**679**	9
Sit in bed	3	1	0	0	0	4	3	13	40	**605**

The number of correctly classified samples for each activity is highlighted in bold

Table 8 The results of leave-five-subjects-out Cross Validation (CV) for each fold with performance metrics: P(recision), R(ecall), F(1-score), Mi(cro avg.), Ma(cro avg.), W(eighted avg.) and A(ccuracy) for the Hospital data set. The predictions are obtained by the CNN-MD and CNN-RD radar-based networks with an ensemble approach

Model	Four-fold	Performance metrics									
	Cross validation	P.W	R.W	F.W	P.Ma	R.Ma	F.Ma	P.Mi	R.Mi	F.Mi	A
CNN-MD	Fold-1	0.90	0.90	0.90	0.86	0.88	0.87	0.90	0.90	0.90	0.90
	Fold-2	0.92	0.91	0.91	0.90	0.90	0.90	0.91	0.91	0.91	0.91
	Fold-3	0.86	0.86	0.86	0.83	0.83	0.83	0.86	0.86	0.86	0.86
	Fold-4	0.90	0.89	0.89	0.84	0.89	0.86	0.89	0.89	0.89	0.89
CNN-RD	Fold-1	0.94	0.94	0.94	0.92	0.94	0.93	0.94	0.94	0.94	**0.94**
	Fold-2	0.96	0.96	0.96	0.95	0.95	0.95	0.96	0.96	0.96	**0.96**
	Fold-3	0.93	0.93	0.93	0.92	0.90	0.91	0.93	0.93	0.93	**0.93**
	Fold-4	0.95	0.95	0.95	0.94	0.94	0.94	0.95	0.95	0.95	**0.95**

The best model accuracy for each fold is highlighted in bold

Table 9 The results of leave-five-subjects-out Cross Validation (CV) using the accuracy metric on the hospital data set. The following models are included: Convolutional Neural Network (CNN), Long Short-Term Memory (LSTM), CNN-LSTM, Support Vector Machine (SVM), Random Forest (RF) and Linear Discriminant Analysis (LDA). The deep learning models are using an ensemble approach for the prediction.

Four-fold CV	Different models accuracy											
	CNN		LSTM		CNN-LSTM		SVM		RF		LDA	
	MD	RD	MD	RD	MD	RD	MD	RD	MD	RD	MD	RD
Fold-1	0.90	0.94	0.85	0.92	0.86	0.94	0.76	0.82	0.67	0.61	0.43	0.79
Fold-2	0.91	0.96	0.88	0.93	0.89	0.94	0.72	0.77	0.68	0.64	0.40	0.75
Fold-3	0.86	0.93	0.86	0.90	0.86	0.93	0.71	0.77	0.64	0.59	0.43	0.74
Fold-4	0.89	0.95	0.87	0.94	0.88	0.95	0.73	0.81	0.69	0.65	0.44	0.78

RD maps for improving the accuracy and the robustness of the models. The results are qualitatively similar (CNN using MD maps outperforms other methods) to [47]. In our results, less sensitivity is observed to the presence or absence of people of different ages (adult people and elderly people) and in the use of mobility aids (with mobility aids and without any aids in the training data set).

The MD signatures are more effective for generalizing across different environments while the RD maps provide a better performance within the same environment. This is because the ability of the model to recognize the activities is mainly based on the velocity/speed of the subjects for each activity performed in the recording environment. In different environments the range dimension is not very useful, and no key discriminative factor, as the range of the activities performed is different in different room setups. Regarding the activities, we observe more confusion among the bed activities and less confusion among the in-room activities. The bed activities are slightly more difficult to recognize compared to other activities. Moreover, the activities are generally better predicted by the models with an ensemble approach.

7 Conclusions and future work

We proposed a novel approach towards automatic recognition of indoor human activities, especially the activities of patients in a hospital room, using various machine learning algorithms and two different radar sensors. In this respect, we collected novel data of patient activities in two different environments. A subset of the data set is made available to the scientific community to encourage further extension of this work. We note that the model generalization is quite good between subjects but quite hard between environments. The MD signature is slightly less sensitive over different environments as the model can not overfit on the range feature (which is significantly different between environments). The RD maps are more effective in a single environment as the range features enable the detection of smaller motions.

In future research, we primarily focus on improving the robustness and generalization of the model. Accordingly, we investigate explainable AI, transfer learning and domain adaptation methods, angle feature (as we suspect angle is an important reason for sensitivity in different environments) and sensor fusion with tracking features.

Appendix: Physical characteristics of the participants involved in Homelab and Hospital data sets.

See the Tables 10 and 11.

Table 10 Homelab data set: physical characteristics of the participants

Nature	Participants					
	No.	Gender	Age	Height (in cm)	Weight (in kg)	Mobility aids
Adult group	1	Female	31	155	47	
	2	Male	30	170	70	
	3	Male	30	180	75	
	4	Female	28	178	56	
	5	Male	37	160	95	Activities performed without any mobility aids
	6	Male	33	174	70	
	7	Male	38	175	74	
	8	Male	27	185	70	
	9	Male	33	178	80	

Table 11 Hospital data set: physical characteristics of the participants. The Elderly people who were not able to perform '*fall on the floor*' and '*stand up from the floor*' activities are indicated with '*' sign in the gender group

Nature	Participants					
	No.	Gender	Age	Height (in cm)	Weight (in kg)	Mobility aids
Adult group	1	Female	28	178	56	Each person performed with and without mobility aids
	2	Male	25	178	73	
	3	Male	30	183	75	
	4	Male	30	180	75	
	5	Male	26	185	72	
	6	Female	31	155	47	
	7	Male	37	160	95	
	8	Male	27	178	80	
	9	Male	24	183	80	
	10	Male	38	175	74	
	11	Male	27	185	70	
	12	Male	25	185	80	
Elderly group	1	Male*	90	172	75	
	2	Female*	82	169	63	
	3	Male	72	175	75	
	4	Female	69	168	68	
	5	Male	74	183	87	
	6	Female*	73	168	65	
	7	Male	85	180	74	
	8	Female	63	175	70	

Acknowledgements The research activities described in this paper were funded by Ghent University-imec and the Flemish Government under the "Onderzoeksprogramma Artificiële Intelligentie (AI) Vlaanderen" programme.

Declarations

Conflict of interest The authors declare that they have no conflict of interest.

References

1. Ageing and Health (2020) https://www.who.int/news-room/fact-sheets/detail/ageing-and-health
2. Zhao M, Li T, Abu Alsheikh M, Tian Y, Zhao H, Torralba A, Katabi D (2018) Through-wall human pose estimation using radio signals. In: 2018 IEEE/CVF conference on computer vision and pattern recognition. IEEE, Salt Lake City, UT, pp 7356–7365
3. Brooker GM (2005) Understanding millimetre wave FMCW radars. In: 1 St international conference on sensing technology. IEEE, New Zealand, pp 152–157
4. Iovescu C, Rao S (2017) The fundamentals of millimeter wave. p 9
5. Chen VC, Li F, Ho SS, Wechsler H (2006) Micro-Doppler effect in radar: phenomenon, model, and simulation study. IEEE Trans Aerosp Electron Syst 42(1):2–21
6. Hong-Bo Zhang, Yi-Xiang Zhang, Bineng Zhong, Qing Lei, Lijie Yang, Ji-Xiang Du, Duan-Sheng Chen (2019) A comprehensive survey of vision-based human action recognition methods. Sensors 19:1005
7. Polfliet V, Knudde N, Vandersmissen B, Couckuyt I, Dhaene T (2018) Structured inference networks using high-dimensional sensors for surveillance purposes. In: Engineering applications of neural networks. Springer International Publishing, pp 1–12
8. Jain DK, Mahanti A, Shamsolmoali P, Manikandan R (2020) Deep neural learning techniques with long short-term memory for gesture recognition. Neural Comput Appl, March
9. Gutoski M, Lazzaretti AE, Lopes HS (2020) Deep metric learning for open-set human action recognition in videos. Neural Comput Appl, June
10. Chao Jing, Ping Wei, Hongbin Sun, Nanning Zheng (2020) Spatiotemporal neural networks for action recognition based on joint loss. Neural Comput Appl 32(9):4293–4302
11. Karpathy A, Toderici G, Shetty S, Leung T, Sukthankar R, Fei-Fei L (2014) Large-scale video classification with convolutional neural networks. In: Proceedings of the 2014 IEEE conference on computer vision and pattern recognition, CVPR '14. IEEE Computer Society, pp 1725–1732
12. Yue-Hei Ng J, Hausknecht M, Vijayanarasimhan S, Vinyals O, Monga R, Toderici G (2015) Beyond short snippets: deep networks for video classification. In: 2015 IEEE conference on computer vision and pattern recognition (CVPR), pp 4694–4702, June
13. Tran D, Bourdev L, Fergus R, Torresani L, Paluri M (2015) Learning spatiotemporal features with 3D convolutional networks. In: The IEEE international conference on computer vision (ICCV), December
14. Zhang Z, Ma X, Song R, Rong X, Tian X, Tian G, Li Y (2017) Deep learning based human action recognition: a survey. In: 2017 Chinese automation congress (CAC), pp 3780–3785, October
15. Herath S, Harandi M, Porikli F (2017) Going deeper into action recognition. Image Vision Comput 60(1):4–21

16. Castro FM, Marín-Jiménez MJ, Guil N, de la Blanca NP (2020) Multimodal feature fusion for CNN-based gait recognition: an empirical comparison. Neural Comput Appl 32(17):14173–14193
17. Feichtenhofer C, Pinz A, Zisserman A (2016) Convolutional two-stream network fusion for video action recognition. In: The IEEE conference on computer vision and pattern recognition (CVPR), June
18. Tsinganos P, Cornelis B, Cornelis J, Jansen B, Skodras A (2020) Hilbert sEMG data scanning for hand gesture recognition based on deep learning. Neural Comput Appl, July
19. Singh T, Vishwakarma DK (2020) A deeply coupled ConvNet for human activity recognition using dynamic and RGB images. Neural Comput Appl, May
20. Falls (2018) https://www.who.int/news-room/fact-sheets/detail/falls
21. Lau SL, König I, David K, Parandian B, Carius-Düssel C, Schultz M (2010) Supporting patient monitoring using activity recognition with a smartphone. In: 2010 7th international symposium on wireless communication systems, pp 810–814, September
22. Ichwana D, Arief M, Puteri N, Ekariani S (2018) Movements monitoring and falling detection systems for transient ischemic attack patients using accelerometer based on internet of things. In: 2018 international conference on information technology systems and innovation (ICITSI), pp 491–496, October
23. Schrader L, Vargas Toro A, Konietzny S, Rüping S, Schäpers B, Steinböck M, Krewer C, Müller F, Güttler J, Bock T (2020) Advanced sensing and human activity recognition in early intervention and rehabilitation of elderly people. J Popul Ageing 13(2):139–165
24. SA Shah, D Fan, A Ren, N Zhao, X Yang, SAK Tanoli (2018) Seizure episodes detection via smart medical sensing system. J Ambient Intell Hum Comput, November
25. Khan Muhammad Bilal, Yang Xiaodong, Ren Aifeng, Al-Hababi Mohammed Ali Mohammed, Zhao Nan, Guan Lei, Fan Dou, Shah Syed Aziz (2019) Design of software defined radios based platform for activity recognition. IEEE Access 7:31083–31088
26. Biagetti G, Crippa P, Falaschetti L, Orcioni S, Turchetti Cl (2018) Human activity monitoring system based on wearable sEMG and accelerometer wireless sensor nodes. BioMed Eng Online 17(Suppl 1):1–18
27. Georgakopoulos SV, Tasoulis SK, Mallis GI, Vrahatis AG, Plagianakos VP, Maglogiannis IG (2020) Change detection and convolution neural networks for fall recognition. Neural Comput Appl, July
28. Aimilia Papagiannaki, Zacharaki Evangelia I, Gerasimos Kalouris, Spyridon Kalogiannis, Konstantinos Deltouzos, John Ellul, Vasileios Megalooikonomou (2019) Recognizing physical activity of older people from wearable sensors and inconsistent data. Sensors 19(4):880
29. Ann-Kathrin Seifert, Amin Moeness G, Zoubir Abdelhak M (2019) Toward unobtrusive in-home gait analysis based on radar Micro-Doppler signatures. IEEE Trans Biomed Eng 66(9):2629–2640
30. Zhu S, Xu J, Guo H, Liu Q, Wu S, Wang H (2018) Indoor human activity recognition based on ambient radar with signal processing and machine learning. In: 2018 IEEE international conference on communications (ICC), pp 1–6, May
31. Yang S, Le Kernec J, Fioranelli F, Romain O (2019) Human activities classification in a complex space using raw radar data. In: 2019 international radar conference (RADAR), pp 1–4, September
32. Linda Senigagliesi, Gianluca Ciattaglia, Adelmo De Santis, Ennio Gambi (2020) People walking classification using automotive radar. Electronics 9(4):588
33. Sevgi Gurbuz, Moeness Amin (2019) Radar-based human-motion recognition with deep learning: promising applications for indoor monitoring. IEEE Signal Process Mag 36:16–28
34. Hao Du, Tian Jin, Yuan He, Yongping Song, Yongpeng Dai (2020) Segmented convolutional gated recurrent neural networks for human activity recognition in ultra-wideband radar. Neurocomputing 396:451–464
35. Lien J, Gillian N, Karagozler M, Amihood P, Schwesig C, Olson E, Raja H, Poupyrev I (2016) Soli: ubiquitous gesture sensing with millimeter wave radar. ACM Trans Graph 35:1–19
36. Wang S, Song J, Lien J, Poupyrev I, Hilliges O (2016) Interacting with soli: exploring fine-grained dynamic gesture recognition in the radio-frequency spectrum. In: Proceedings of the 29th annual symposium on user interface software and technology, UIST '16. ACM, pp 851–860
37. Vandersmissen B, Knudde N, Jalalvand A, Couckuyt I, Dhaene T, De Neve W (2019) Indoor human activity recognition using high-dimensional sensors and deep neural networks. Neural Comput Appl, August
38. Fioranelli F, Shah SA, Li H, Shrestha A, Yang S, Le Kernec J (2019) Radar sensing for healthcare. Electron Lett 55(19):1022–1024
39. Chuanwei Ding, Hong Hong Yu, Chu Zou Hui, Xiaohua Zhu, Francesco Fioranelli, Julien Le Kernec, Changzhi Li (2019) Continuous human motion recognition with a dynamic range-Doppler trajectory method based on FMCW radar. IEEE Trans Geosci Remote Sens 57(9):6821–6831
40. Zhao H, Hong H, Miao D, Li Y, Zhang H, Zhang Y, Li C, Zhu X (2019) A noncontact breathing disorder recognition system using 2.4-GHz digital-IF Doppler radar. IEEE J Biomed Health Inform 23(1):208–217
41. Fioranelli F, Le Kernec J, Shah SA (2019) Radar for health care: recognizing human activities and monitoring vital signs. IEEE Potent 38(4):16–23
42. Shah SA, Fioranelli F (2019) Human activity recognition: preliminary results for dataset portability using FMCW radar. In: 2019 international radar conference (RADAR), pp 1–4, September
43. Gurbuz SZ, Clemente C, Balleri A, Soraghan JJ (2017) Micro-Doppler-based in-home aided and unaided walking recognition with multiple radar and sonar systems. IET Radar Sonar Navigat 11(1):107–115
44. Haobo Li, Aman Shrestha, Hadi Heidari, Julien Le Kernec, Francesco Fioranelli (2020) Bi-LSTM network for multimodal continuous human activity recognition and fall detection. IEEE Sens J 20(3):1191–1201
45. Branka Jokanović, Moeness Amin (2018) Fall detection using deep learning in range-Doppler radars. IEEE Trans Aerosp Electron Syst 54(1):180–189
46. Haobo Li, Aman Shrestha, Hadi Heidari, Julien Le Kernec, Francesco Fioranelli (2019) Magnetic and radar sensing for multimodal remote health monitoring. IEEE Sens J 19(20):8979–8989
47. Jia M, Li S, Le Kernec J, Yang S, Fioranelli F, Romain O (2020) Human activity classification with radar signal processing and machine learning. In: 2020 International conference on UK-China emerging technologies (UCET), pp 1–5, August
48. Fioranelli F, Shah SA, Li H, Shrestha A, Yang S, Le Kernec J (2019) Radar signatures of human activities. http://researchdata.gla.ac.uk/848/. https://doi.org/10.5525/gla.researchdata.848, July
49. Ritchie M, Capraru R, Fioranelli F (2020) Dop-NET: a micro-Doppler radar data challenge. Electron Lett 56, February
50. Baptist Vandersmissen, Nicolas Knudde, Azarakhsh Jalalvand, Ivo Couckuyt, André Bourdoux, Wesley De Neve, Tom Dhaene (2018) Indoor person identification using a low-power FMCW radar. IEEE Trans Geosci Remote Sens 56(7):3941–3952

51. Jri Lee, Yi-An Li, Meng-Hsiung Hung, Shih-Jou Huang (2010) A fully-integrated 77-GHz FMCW radar transceiver in 65-nm CMOS technology. IEEE J Solid State Circuits 45(12):2746–2756
52. Chen Q, Tan B, Chetty K, Woodbridge K (2016) Activity recognition based on micro-Doppler signature with in-home Wi-Fi. In: 2016 IEEE 18th international conference on E-Health networking, applications and services (Healthcom), pp 1–6, September
53. Chang C-C, Lin C-J (2011) LIBSVM: a library for support vector machines. ACM Trans Intell Syst Technol 2(3):27:1-27:27
54. Leo Breiman (2001) Random forests. Mach Learn 45(1):5–32
55. Alex Krizhevsky, Ilya Sutskever, Hinton Geoffrey E (2017) ImageNet classification with deep convolutional neural networks. Commun ACM 60(6):84–90
56. Nair V, Hinton GE (2010) Rectified linear units improve restricted Boltzmann machines. In: Fürnkranz J, Joachims T (eds) Proceedings of the 27th international conference on machine learning (ICML-10). Omnipress, pp 807–814
57. Glorot X, Bordes A, Bengio Y (2011) Deep sparse rectifier neural networks. In: Proceedings of the fourteenth international conference on artificial intelligence and statistics, pp 315–323, June
58. Clevert D-A, Unterthiner T, Hochreiter S (2016) Fast and accurate deep network learning by exponential linear units (ELUs). arXiv:1511.07289 [cs], February